International Journal of Thermophysics, Vol. 9, No. 5, 1988

Thermal Conductivity and Thermal Expansion of Stainless Steels D9 and HT9[1]

L. Leibowitz[2] and R. A. Blomquist[2]

Renewed interest in the use of metallic fuel in a liquid–metal fast breeder reactor has prompted study of the thermodynamic and transport properties of fuel and cladding materials. Two stainless steels are of particular interest because of their good performance under irradiation. These are D9, an austenitic steel, and HT9, a ferritic steel. Thermal conductivity and thermal expansion data for these cladding alloys are of particular interest in assessing in-reactor behavior. These two properties were measured for the two steels at temperatures to 1200 K. Of particular interest is the influence on these properties of a phase transition in HT9.

KEY WORDS: high temperature; phase transition; stainless steel; thermal conductivity; thermal expansion.

1. INTRODUCTION

Recently, increased interest in metallic (U–Pu–Zr) fuel for liquid–metal fast breeder reactors [1] has prompted a reassessment of the available thermodynamic and transport property data for materials of interest. The two primary cladding alloys under consideration are the stainless steels D9, an austenitic alloy, and HT9, a ferritic alloy.

Modeling of fuel performance and reactor behavior depends, in part, on the thermodynamic and transport properties of the cladding. Because of a lack of reliable literature data for D9 and HT9, we undertook measurements of their thermal expansion and thermal conductivity. Our results are reported below.

[1] Paper presented at the Tenth Symposium on Thermophysical Properties, June 20–23, 1988, Gaithersburg, Maryland, U.S.A.

[2] Chemical Technology Division, Argonne National Laboratory, 9700 South Cass Avenue, Argonne, Illinois 60439, U.S.A.

0195-928X/88/0900-0873$06.00/0

2. EXPERIMENTAL

2.1. Materials

The cladding alloys studied were D9, an austenitic steel similar to 316 stainless steel, and HT9, a ferritic alloy, similar to 400 series steels. The composition for D9 is 15.5 wt% Ni, 13.5 wt% Cr, 2.0 wt% Mn, 2.0 wt% Mo, 0.75 wt% Si, 0.25 wt% Ti, and 0.04 wt% C; the composition for HT9 is 0.5 wt% Ni, 12.0 wt% Cr, 0.2 wt% Mn, 1.0 wt% Mo, 0.25 wt% Si, 0.5 wt% W, 0.5 wt% V, and 0.2 wt% C, with the balance Fe. The alloys were used in the as-received condition. The D9 was solution annealed at 1322 K and 20% cold worked; the HT9, which had a martensitic structure, was tempered by heat treating at 1311 and at 1033 K.

2.2. Thermal Expansion

The thermal expansion of the alloys was measured with a Netzsch Inc. Model 402 dilatometer containing a horizontal, single push rod and a rhodium furnace. Because it was used for measurements on plutonium-containing materials, the instrument was located in a helium-atmosphere glove box and connected to a KineticSystems Corp. Computer Automated Measurement and Control (CAMAC) data acquisition system which was interfaced to a Digital Equipment Corp. (DEC)PDP-11/34 computer. The sample was held in an alumina support tube, closed at one end, and positioned in the center of the constant temperature zone of the furnace. A vacuum-tight protective tube allowed control of the atmosphere to which the sample was exposed. An alumina rod in a low-friction support transferred the change in length of the sample to an inductive displacement transducer. Sample temperatures were measured with a Type S (Pt vs Pt–10% Rh) thermocouple.

In a typical measurement, a 50-mm-long sample was prepared with flat, parallel end faces and installed in the instrument. The furnace was evacuated and flushed with high-purity helium several times and finally filled with high-purity helium to a pressure slightly above ambient. The desired set of temperature cycles was entered in the temperature controller, and the test series begun. The dilatometer was periodically calibrated with an NBS tungsten thermal expansion standard (SRM 737). A variety of heating and cooling rates was tested, and 1 $K \cdot min^{-1}$ was chosen as the standard rate. A few measurements made on HT9 at 0.5 and 2 $K \cdot min^{-1}$ are discussed below. Length changes measured with the dilatometer depend on the differences between the expansion of the sample and that of its holder. From the known thermal expansion of the NBS standard, a correction due to expansion of the sample holder was calculated and applied

to subsequent measurements. Separate temperature calibrations were performed using NBS aluminum (SRM 44f) and high-purity gold (reported to be 99.99% pure). These calibrations were performed by using a foil of the metal between two 25.4-mm-long alumina rods in place of the normal thermal expansion sample. The temperature at which a sharp change in length was observed was taken as the melting point of the metal. In all cases, our indicated temperatures were within ± 2 K of the expected melting point. We estimated the accuracy of our thermal expansion data to be about $\pm 2\%$, although the precision is significantly better (discussed later).

2.3. Thermal Conductivity

The thermal conductivity was measured with a Dynatech Corp. Model TCFCM-N20 thermal conductivity instrument. The instrument was located in the same helium-atmosphere glove box as the thermal expansion system. The hot zone of the instrument was further protected from gaseous impurities by enclosing it in a large aluminum bell jar, secured to the base plate through a rubber gasket. The bell jar could be evacuated and filled with high-purity helium. The apparatus is based on the comparative thermal conductivity method [2]. An unknown cylindrical sample was positioned under spring compression between two identical, calibrated reference cylinders, thereby forming a vertically stacked column. Longitudinal heat flow was established by heaters placed above and below the column. The bottom heater rested on a water-cooled block and served as a heat sink. Radial heat losses were minimized by surrounding the column with guard furnaces in which the thermal gradient was matched to that of the column and by filling the annular space with alumina granules.

Six ungrounded Chromel–Alumel thermocouples sheathed in Inconel were used for temperature measurements. Each of the three cylinders comprising the experimental stack held two thermocouples in wells that were a known distance apart. No thermocouple calibrations were made because only the differences in temperature were of consequence in calculating thermal conductivities and because all thermocouples were derived from the same batch. In earlier work with this instrument, thermocouple calibrations were performed and corrections were found to be negligible.

In a typical experiment, the column was assembled and the thermocouples were inserted into their designated wells. After the guard furnace had been lowered, the annular space was filled with alumina granules and covered with quartz wool. After the bell jar had been lowered on the base plate, the assembly was evacuated, degassed for several hours at 572 K, flushed several times with ultrahigh-purity helium, and then backfilled with helium to a pressure of ~ 80 kPa. The top and bottom heaters

were programmed for the desired temperature gradient (~ 80 K), and the system was allowed to come to steady state. At the end of equilibration, thermocouple outputs were measured with a digital voltmeter to within $\pm 5\ \mu$V, and the heaters were reprogrammed for the next temperature.

Our experience indicated that slight heat flux (q_i) differences, noticeable between the top and the bottom references, are functions of the total temperature gradient (ΔT) imposed on the column between the top and the bottom thermocouples. In earlier measurements, we attempted to improve the accuracy of our data by obtaining at least two values of ΔT selected in such a way that the condition $q_{\text{top}} > q_{\text{bottom}}$ existed at the lower ΔT value and $q_{\text{top}} < q_{\text{bottom}}$ at the higher value. Linear interpolations (or, in some cases, extrapolations) were then used to establish a value of ΔT at which there was an identical heat flux (q_{ref}) in both references and also to determine the corresponding average value of the sample temperature centered between the thermocouples in the unknown. Thermal conductivity of the unknown sample was then calculated from the following equation:

$$\lambda_{\text{sample}} = \left(\frac{\Delta x}{\Delta T}\right)_{\text{sample}} \left(\lambda \frac{\Delta T}{\Delta x}\right)_{\text{ref}} \tag{1}$$

Subsequent measurements showed that no improvement in reliability was gained by using this procedure. In the work described here, we used only a single gradient at which differences in heat fluxes in the top and bottom references were insignificant.

The primary reference standard used for the thermal conductivity measurement was austenitic stainless steel (SRM 1462) supplied by the National Bureau of Standards (NBS). Its chemical composition is 62.0 wt% Fe, 20.2 wt% Ni, 16.2 wt% Cr, 1.2 wt% Mn, 0.28 wt% Si, and <0.01 wt% C.

Cylindrical samples (25.4 mm in diameter and 25.4 mm high) were machined from available stock, and thermocouple wells (12.7 mm long and 1.7 mm in diameter) were drilled 6.35 mm from the top and bottom of each sample. The faces of the samples were carefully polished to provide good thermal contact.

Thermal expansion corrections were made to the interwell distances of all alloys used. Our own thermal expansion values were used for the cladding alloys D9 and HT9. For the NBS reference, data were taken from the compilation by Touloukian et al. [34], substituting Fe + 24–26 wt% Ni + 15–20 wt% Cr + $\sum x_i$ for the NBS standard. Thermal expansion corrections between room temperature and 1200 K were 1.4% for the NBS reference, 1.8% for D9, and 1.1% for HT9.

Test measurements were performed in which all three cylinders were

NBS reference steel; that is, we measured the thermal conductivity of the NBS standard in the same way we would measure our unknown alloys. These measurements were within the NBS stated uncertainty of 5%. We estimated the accuracy of our measurements on cladding alloys to be about ±10%, although the precision is significantly better (discussed later).

3. RESULTS

3.1. Thermal Expansion

3.1.1. D9

Figure 1 shows thermal expansion data for D9 as well as data for 316 stainless steel of a similar composition reported by Lucks et al. [4] and data given by Touloukian et al. [3] for 300 series stainless steels, including 316. No data are available in the literature for the thermal expansion of D9. The composition of the steel used by Lucks et al. [4] was 11.6 wt% Ni, 16.82 wt% Cr, 1.59 wt% Mn, 2.18 wt% Mo, 0.26 wt% Si, 0.108 wt% C, 0.023 wt% S, and 0.018 wt% P, with the balance Fe. One point tabulated at 1123 K in Ref. 4, which appears to have been a typographical error, was omitted from the plot. As can be seen in Fig. 1, the agreement between the three sets of data is good, and in contrast with HT9 (as

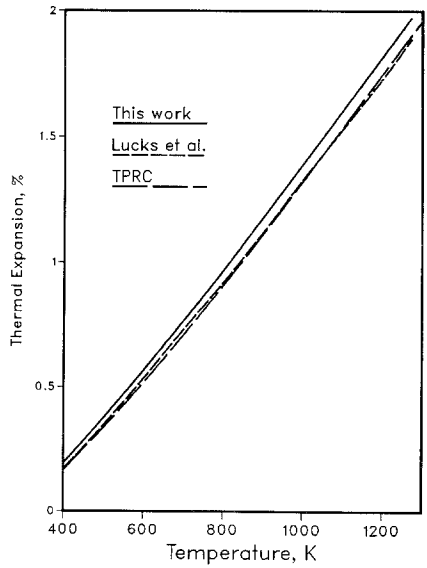

Fig. 1. Thermal expansion of D9 compared with data of Lucks et al. [4] and Touloukian et al. [3] (TPRC) for 316 stainless steel.

discussed below), no phase transitions are apparent. The key features of present interest in these steel alloys are the existence of an fcc γ phase (austenite) and a bcc α phase (ferrite). An inspection of the Fe–Cr–Ni phase diagram [5] suggests no transitions from the γ phase in D9. Our thermal expansion results for the heating and cooling cycles agreed very well for this alloy. The pooled results of six heating and cooling cycles at $1\ \mathrm{K} \cdot \mathrm{min}^{-1}$ are described by Eq. (2) (in the range 400–1300 K) with a percentage standard deviation (σ) of 0.17.

$$\Delta L/L_0 = -0.4247 + 1.282 \times 10^{-3} T + 7.362 \times 10^{-7} T^2 - 2.069 \times 10^{-10} T^3 \quad (2)$$

In Eqs. (2) and (3), the temperature, T, is in K, and the relative change in length referenced to 293 K is given as a percentage. That is, $\Delta L/L_0 = 100 \times [L(T) - L(293)]/L(293)$.

3.1.2. HT9

Thermal expansion data for HT9 are shown in Fig. 2. It is evident that a transition occurs at about 1100 K on heating and about 1050 K on cooling.

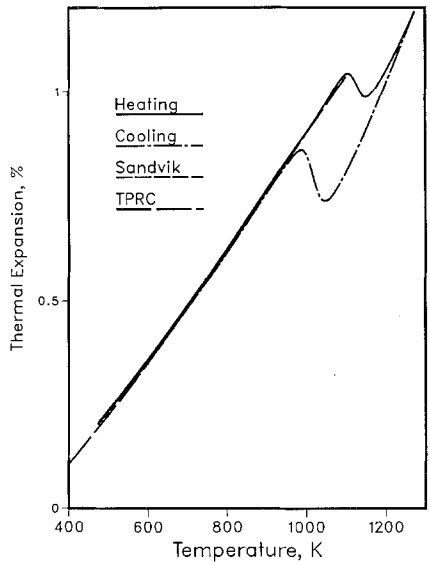

Fig. 2. Thermal expansion of HT9 compared with data given for HT9 by SANDVIK [7] and for 410 stainless steel by Touloukian et al. [3] (TPRC); "heating" and "cooling" designate data obtained by us for heating and cooling cycles.

Inspection of the Fe–Cr–Ni [5] and the Fe–Cr phase diagrams [6] indicates that a $\alpha \rightarrow \gamma$ transition would be expected at roughly 1100 K. On cooling, however, the transition is substantially delayed, even at $1\,\mathrm{K}\cdot\mathrm{min}^{-1}$. A few measurements were performed at rates of 0.5 and $2\,\mathrm{K}\cdot\mathrm{min}^{-1}$. Results were essentially identical at 0.5 and $1\,\mathrm{K}\cdot\mathrm{min}^{-1}$, whereas markedly increased hysteresis was found at $2\,\mathrm{K}\cdot\mathrm{min}^{-1}$.

With regard to the Fe–Cr–Ni phase diagram, Ref. 5 states that "the outstanding feature, however, is the pronounced reluctance of metastable austenite to transform when once established at high temperatures." The hysteresis shown in Fig. 2 clearly demonstrates this effect. Also shown in Fig. 2 are data for the thermal expansion of HT9 taken from an industrial data sheet [7] and from values given by Touloukian et al. for 400 series stainless steels, including 410, which is similar to HT9. The agreement of Refs. 7 and 3 with our results at low temperatures is very good. Equation (3) ($\sigma = 0.17$) represents our data below the transition temperature (in the range 400–1090 K in heating and 400–990 K in cooling).

$$\Delta L/L_0 = -0.2191 + 5.678 \times 10^{-4} T + 8.111 + 10^{-7} T^2 - 2.576 \times 10^{-10} T^3 \quad (3)$$

3.2. Thermal Conductivity

3.2.1. D9

There are no literature values for the thermal conductivity of D9. Thus, our measured thermal conductivity data for D9 are compared in Fig. 3 with literature values for 316 stainless steel [4, 8, 9]. As can be seen, agreement is quite good with the data of Lucks et al. [4]. At higher temperatures, our data differ somewhat with the data of Matolich [8] and Chu and Ho [9]. The composition of Matolich's sample of 316 stainless steel (his designation 3A) was 12.60 wt% Ni, 17.45 wt% Cr, 1.59 wt% Mn, 2.55 wt% Mo, 0.6 wt% Si, 0.063 wt% C, 0.01 wt% S, 0.023 wt% P, 0.09 wt% Cu, and 0.19 wt% Co, with the balance Fe. The values of Chu and Ho arose from an assessment of a great many measurements on 316 stainless steel. Considering the accuracy of the measurements plotted in Fig. 3, the differences are of marginal significance.

Our data for D9 were taken in random temperature order to minimize any influence of instrument drift or other sources of systematic error. There seems to be a change in our data at about 1030 K which, because of the precision of our data, we believe to be real. We have, consequently, represented the values in the range 500–1030 K by Eq. (4) ($\sigma = 0.47$) and values in the range 1030–1200 K by Eq. (5) ($\sigma = 0.51$).

$$\lambda = 7.598 + 2.391 \times 10^{-2} T - 8.899 \times 10^{-6} T^2 \quad (4)$$

$$\lambda = 7.260 + 1.509 \times 10^{-2} T \quad (5)$$

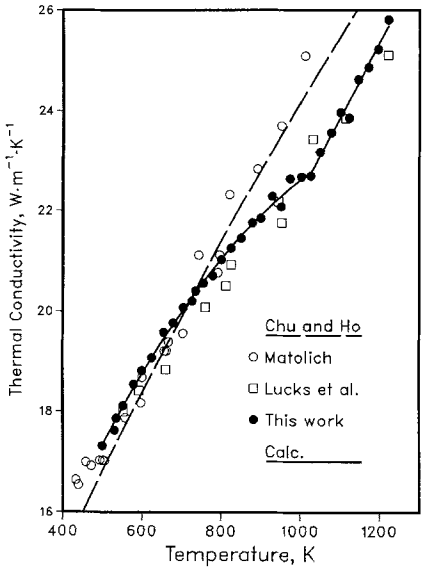

Fig. 3. Thermal conductivity of D9 compared with data for 316 stainless steel of Matolich [8], Lucks et al. [4], and Chu and Ho [9].

The thermal conductivity, λ, is in $W \cdot m^{-1} \cdot K^{-1}$ and the temperature, T, is in K.

3.2.2. HT9

Figure 4 shows our data for the thermal conductivity of HT9 along with values taken from an industrial data sheet for HT9 [7] and the values recommended by Chu and Ho [9] for 410 stainless steel. Agreement is reasonable good with the smoothed curve obtained from the SANDVIK [7] values; however, these values are quite sparse. Agreement with the Chu and Ho values is also fairly good, considering that they apply to different steels. Chu and Ho comment that there are no data for temperatures above 1000 K, and their recommended values above that temperature are based on extrapolations. Our experience has shown that it is extremely difficult to obtain reproducible data much above that temperature. Reproducible values could be obtained in random temperature order either entirely below or entirely above the transition temperature. It was very difficult, however, to move from above to below the transition temperature and reproduce the lower temperature data. This could be done only by changing the temperature in very small steps and waiting for long times

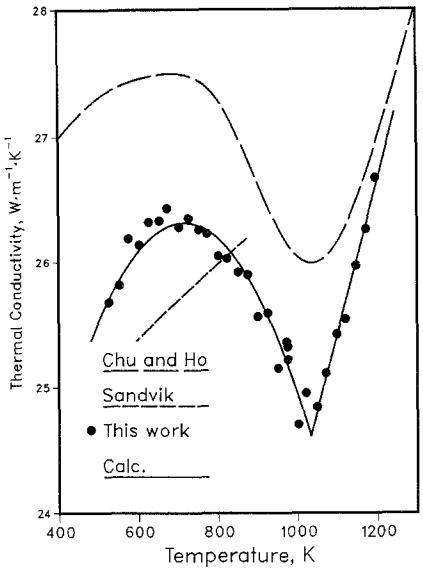

Fig. 4. Thermal conductivity of HT9 compared with data given for HT9 by SANDVIK [7] and for 410 stainless steel by Chu and Ho [9].

before measuring the conductivity. Obtaining reproducible results by moving from below to above the transition was simpler, in accord with expectations for the ferritic-to-austenitic transformation. Equation (6) ($\sigma = 0.57$) represents our data below the transition in the range 500–1030 K, and Eq. (7) reproduces the data ($\sigma = 0.30$) in the range 1030–1200 K.

$$\lambda = 17.622 + 2.428 \times 10^{-2} T - 1.696 \times 10^{-5} T^2 \quad (6)$$

$$\lambda = 12.027 + 1.218 \times 10^{-2} T \quad (7)$$

The thermal conductivity, λ, is in $\mathrm{W \cdot m^{-1} \cdot K^{-1}}$ and the temperature, T, is in K.

4. DISCUSSION

The thermal expansion results for D9 and HT9 are in reasonable accord with expectations from the relevant phase diagrams [5, 6]. No transitions that would influence thermal expansion are expected in the austenitic alloy, D9. In contrast, the ferritic steel, HT9, is expected to show

a ferritic-to-austenitic transition in the neighborhood of 1100 K. Curie transitions would not influence thermal expansion. The hysteresis shown by the thermal expansion data for HT9 is a reflection of the difficulty of reversing the phase transition.

The thermal conductivity results are somewhat more difficult to interpret. It is expected that a Curie transition influences the thermal conductivity at high temperatures. In the ferritic alloys, one would be expected at a temperature of about 1040 K, slightly below that of the $\alpha \rightarrow \gamma$ transition. Indeed, we found a marked break in the thermal conductivity data for HT9 at about 1030 K rather than at the 1100 K seen in expansion. Only one thermal conductivity measurement was obtained between these temperatures (at 1071 K), and we cannot distinguish between the effect of the $\alpha \rightarrow \gamma$ and that of the Curie transition on thermal conductivity. It is possible that the thermal expansion transition at 1100 K was slightly delayed. Thermal expansion measurements at heating rates lower than $0.5\ \mathrm{K} \cdot \mathrm{min}^{-1}$, which could elucidate this possibility, could not be performed. However, because virtually identical results were obtained at 0.5 and $1\ \mathrm{K} \cdot \mathrm{min}^{-1}$, work at even lower rates does not seem promising. The observation of a transition in the D9 thermal conductivity data at 1030 K, exactly the same temperature as seen in HT9, leads us to speculate that a small amount of a ferritic phase had been formed in that alloy, possibly as a consequence of the heat treatment it received during the thermal conductivity measurements. Because the sample used is now contaminated with plutonium, further examination will be very difficult. A similar effect may be responsible for the differences between the data of Lucks et al. [4] and those of Matolilch [8].

5. SUMMARY

Data have been presented for thermal expansion and thermal conductivity of the steel alloys D9 and HT9. The austenitic alloy, D9, shows values for both thermal expansion and thermal conductivity typical of 316 stainless steel. The ferritic alloy, HT9, however, shows a phase transition in the neighborhood of 1030 K and is similar to 410 stainless steel in these properties. Although 1030 K is far above the recommended service temperature of HT9, assessments of its behavior under severe, unexpected conditions, such as hypothetical nuclear reactor accidents, must take this transition into account.

ACKNOWLEDCGMENTS

This work was supported by the U.S. Department of Energy. The authors wish to express their appreciation to Professor G. R. Speich, Illinois Institute of Technology, for his helpful comments on the metallurgy of steel.

REFERENCES

1. Leon C. Walters, B. R. Seidel, and J. H. Kittel, *Nucl. Tech.* **65**:179 (1984).
2. J. Francl and W. D. Kingery, *J. Am. Ceram. Soc.* **37**:80 (1954).
3. Y. S. Touloukian, R. W. Powell, C. Y. Ho, and P. G. Klemens, *Thermophysics Properties of Matter, Vol. 12, Thermal Expansion* (IFI/Plenum, New York, 1970).
4. C. F. Lucks, H. B. Thompson, A. R. Smith, F. P. Curry, H. W. Deem, and G. F. Bing, United States Air Force Technical Report, USAF-TR-6145-1 (Feb. 1951).
5. ASM, *Metals Handbook, Vol. 8. Metallography, Structure, and Phase Diagrams*, 8th ed. (American Society for Metals, Menlo Park, Ohio, 1973), p. 425.
6. R. Hultgren, P. D. Desai, D. T. Hawkins, M. Gleiser, and K. K. Kelley, *Selected Values of the Thermodynamic Properties of Binary Alloys* (American Society for Metals, Menlo Park, Ohio, 1973), p. 696.
7. SANDVIK, SANDVIK data sheet, SANDVIK HT9, S-1720-ENG (May 1981).
8. J. Matolich, Jr., Battelle Memorial Institute Report, BATT-7096 (Sept. 1965) (also NASA-CR-54151).
9. T. K. Chu and C. Y. Ho, *Proc. 15th Int. Conf. Therm. Conduct.*, V. V. Mirkovich, ed. (Plenum, New York, 1978), p. 79.